Inverse characterization method of viscoelastic materials using dispersion analysis

T. Bourgana [1,2,4], **R. F. Boukadia** [1,3,4], **S. Jonckheere** [1,4], **C. Claeys** [1,4], **G. Chevallier** [2], **M. Ouisse** [2], **E. Deckers** [1,4]

[1] KU Leuven, Department of Mechanical Engineering,
Celestijnenlaan 300 B, B-3001, Heverlee, Belgium
e-mail: **taoufikmohamed.bourgana@kuleuven.be**

[2] FEMTO-ST, Applied Mechanics Department, UMR-CNRS 6174,
24 chemin de l'épitaphe, 25000 Besançon, France.

[3] LTDS UMR-CNRS 5513, École Centrale de Lyon,
36 avenue Guy de Collongue, 69134 Écully, France.

[4] Flanders Make DMMS lab.

Abstract

This paper presents a dispersion-based method for identifying visco-elastic material properties by minimizing the residue between data of virtual experiments and data based on a viscoelastic model through the use of surrogate modeling. The dispersion data retrieved from a virtual experiment of a finite beam with constrained layer damping (the real and imaginary part of the wavenumber) is fitted with numerical dispersion data through an optimization scheme, which can be computationally expensive. In order to alleviate this issue, attention has been focused on the construction of a surrogate model that makes the optimization scheme cheaper without loosing much accuracy in the prediction. This paper uses an interpolation method based on radial basis functions. Once the surrogate model is constructed, the viscoelastic parameters can then be identified and results are compared to the reference parameters.

1 Introduction

Lightweight structures are increasingly used in many industrial sectors for their high stiffness to mass ratio. However, this comes with the price of deteriorated NVH performance. A common way to solve this issue is to use visco-elastic materials usually incorporated in two configurations : constrained and unconstrained visco-elastic layers, meaning that the visco-elastic core is bonded between a host and a constraining structure in the former case, in the latter case the visco-elastic core is directly put on the host structure. These materials are often desirable for their ability to dissipate part of the vibrational energy by heat when they are constrained in shear loading, e.g. when they are constrained by the host structure as well as the constraining layer [1].

In order to run numerical simulations to assess the performance of visco-elastic materials on a given vibrating structure, an accurate knowledge of its parameters is necessary. Several characterization techniques exist to identify the complex frequency-dependent properties of this class of materials, amongst them the dynamical mechanical analysis [3] and the Oberst beam test [4] are the most commonly used. The former is a quasi-static method (low frequencies) and the latter is a resonant method where only the first modes of the tested beam are taken into account. Both techniques are based on the assumption that the visco-elastic material

is rheologically simple, meaning that the time-temperature superposition[3] can be applied in order to extrapolate the storage and loss modulus of the viscoelastic material to higher frequencies. However, for some materials such as polymeric blends, the time-temperature superposition principle is no longer applicable, and thereby a new characterization technique which is not based on this principle is needed. In [2] several experimental identification methods were presented, ranging from quasi-static to higher frequencies, and were then compared to DMA measurements. It has been shown that although results using different methods were coherent, it is not easy to obtain a continuous description of the viscoelastic behavior of a material in the frequency range $[500, 5000]$ Hz. Another method has been presented in [5] and takes advantage of surface (Rayleigh) waves propagating in a infinite half-space visco-elastic material to retrieve experimentally, by means of an inverse technique, the material parameters. Two approaches have been proposed for the identification: on the one hand, a visco-elastic model type is assumed and updated in an optimization scheme such that numerical surface wave speed matches the measured one, on the other hand a similar model updating scheme is carried out but using frequency response function fitting instead. However, the theory is based on the premise that the visco-elastic material is considered as an infinite half-space whereas the experimental setup has finite boundaries, which explains the discrepancies noticed and stated by the authors. A reliable, simple, but not trivial, identification technique has been presented in [7] to characterize rod-like visco-elastic materials when they are subjected to longitudinal harmonic solicitation. It uses the Fourier Transform on experimental data of wave pulse propagating in a long 1D structure. This method provides very good results in determining visco-elastic properties in a wide frequency range, without making any assumption whether or not the material is rheologically simple. It is used when the rod is long enough and the attenuation of propagating waves is sufficiently high. Nonetheless, if right and left going waves are both contributing to the displacement field, meaning existence of reflected waves due to boundary conditions, the method will no longer be applicable. In [8] two techniques have been presented allowing the experimental identification of the equivalent complex frequency-dependent bending stiffness and damping of multi-layer plates : the force analysis technique [9] and a wave fitting technique by means of Hankel's function image source model [10], the output of these methods (equivalent material properties) were fitted with Guyader's homogenization model [11] or Ross, Kerwin and Ungar's model [12] in order to find the frequency-dependent properties of the damping layer.

Yet another inverse technique for the identification of linear visco-elastic material has been suggested in the literature. It is based on the minimization of the residual between measured data and numerical finite element model data. The latter is updated through an optimization scheme by varying the visco-elastic model parameters : Generalized Maxwell [13, 14], fractional derivatives [15]. The minimization can be modal-based [16] as well as frequency response function-based [17]. This technique has been widely applied in the literature, for instance in [17] for 1D structures, or in [18, 19, 20] for 2D structures. Although this type of method has several advantages, the hurdle comes up when dealing with highly damped structures where the identification of the modal parameters becomes really delicate, which is usually the case for high order modes where the behavior of the structure is local.

To amend to this issue, a new inverse characterization technique is hereby proposed. It is based on minimizing the distance between experimental and predicted dispersion curves from a wave finite element model through an optimization scheme. The experimental data in this case are replaced by numerical dispersion curves with added noise. The proposed method is applied to a highly damped beam treated with constrained layer damping, and the visco-elastic material parameters are identified using the proposed method over a broad frequency range.

This paper is structured as follows : in section 2, a viscoelastic model will be discussed, the latter will be used in section 3 in modeling the treated beam using the wave finite element method. McDaniel's method will be discussed as well in the same section. Finally, in section 4, an identification procedure will be presented through the use of surrogate modeling.

2 Linear viscoelastic behavior

Viscoelastic materials are known to dissipate vibrational energy, in particular when performing under shear stress. They possess both viscous and elastic behavior, and consequently their modulus is represented, in the frequency domain, by a complex quantity satisfying the following constitutive equation :

$$\tilde{\sigma}(\omega) = E_\nu(\omega)\tilde{\epsilon}(\omega), \tag{1}$$

where $\tilde{\sigma}$ and $\tilde{\epsilon}$ are the stress and strain expressed in the frequency domain, respectively. The frequency-dependent complex modulus of the visco-elastic material is written as :

$$E_\nu(\omega) = E'(\omega) + iE''(\omega) = E'(\omega)(1 + i\eta(\omega)), \tag{2}$$

The real part $E'(\omega)$, also known as the storage modulus, relates to the elastic behavior of the material, and defines its stiffness. The imaginary part $E''(\omega)$, also known as the loss modulus, relates to the material viscous behavior, and defines its energy dissipating ability of the material, the relationship between the storage modulus and the loss modulus can also be defined through the loss factor $\eta(\omega)$. One of the characteristics of viscoelastic materials is that their properties are influenced by many parameters, such as : frequency, temperature, dynamic strain rate, static pre-load, time effects such as creep and relaxation, aging and other irreversible effects [3]. The material complex modulus is dependent on all these factors. however, frequency and temperature are the most important.

Fractional derivative model:

The fractional derivative model is used to characterize the behavior of visco-elastic materials in frequency and time domain. The four-parameter fractional derivative model, also known as the generalized Zener model is given by the fractional differential equation as :

$$\sigma(t) + \tau^\alpha \frac{d^\alpha \sigma(t)}{dt^\alpha} = E_0\epsilon(t) + \tau^\alpha E_\infty \frac{d^\alpha \epsilon(t)}{dt^\alpha}, \tag{3}$$

where E_0 and E_∞ are the static and high frequency modulus respectively, τ is the relaxation time and α is the fractional parameter.

By applying a Fourier transform to equation (3), one can find the complex modulus of the viscoelastic material in the frequency domain, which is the ratio between the stress and the strain, as :

$$E_\nu(\omega) = \frac{E_0 + E_\infty(i\omega\tau)^\alpha}{1 + (i\omega\tau)^\alpha}. \tag{4}$$

This fractional derivative model is used in the following as it enables characterization of a wide variety of visco-elastic materials with only four parameters.

3 Modeling and numerical experiment

A modeling procedure and experimentation process are necessary for the parameter estimation. In the following, a wave finite element model of a segment of a treated beam will be presented as well as a specific numerical experimentation to identify dispersion curves.

The virtual test case is schematically represented in fig. 1 :

Figure 1: Representation of the clamped treated beam and excitation location

The constrained layer beam shown in fig. 1 is clamped at one end and excited at the other with a point force, the host structure as well as the constraining layer are in steel (shown in black in fig. 1), the viscoelastic material (shown in blue in fig. 1) parameters to be identified as well as the chosen steel properties are shown in table (1), the length of the beam in the $\vec{x}$ direction is $L = 0.6$ m, and $b = 0.03$ m in the $\vec{y}$ direction, the thickness in the $\vec{z}$ direction are $t_1 = 0.004$ m, $t_2 = 0.001$ m and $t_3 = 0.001$ m for the host structure, the viscoelastic core and the constraining layer respectively.

Parameters	Values	Units
E_0	10^6	[Pa]
τ	10^{-6}	[s]
α	0.6	[-]
E_∞	10^{10}	[Pa]
E_{steel}	$2.1\ 10^{11}$	[Pa]
ν_{steel}	0.3	[-]
ν_{visco}	0.37	[-]
ρ_{steel}	7850	[kg/m^3]
ρ_{visco}	990	[kg/m^3]

Table 1: Material properties of the three-layered beam

3.1 Wave finite element model

The Wave Finite Element method is a technique to investigate wave motion in periodic structures. It enables the dispersion analysis of a periodic structure by only studying one period or segment of it, which saves computation time.

A small segment of length $L = 0.01$ m of the treated beam previously shown in fig. 1, is considered and meshed using finite elements. Solid elements are used for the visco-elastic core and shell elements for the faces (see fig. 2).

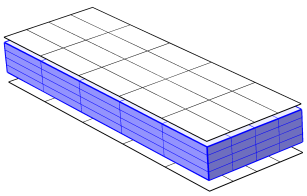

Figure 2: Finite element model of the unit cell of the treated beam

Once discretized, the equation of motion of the isotropic treated beam can be written as :

$$[\mathbf{K}^{(e)} + E_\nu(\omega)\mathbf{K}^{(\nu)} - \omega^2\mathbf{M}]\mathbf{q} = \mathbf{F}, \tag{5}$$

where $\mathbf{K}_e$, $\mathbf{K}_\nu$ and $\mathbf{M}$ are the global stiffness matrix associated with the elastic part of the structure, the global stiffness matrix associated with the viscoelastic part and evaluated at a unitary modulus and the global mass matrix, respectively. $E_\nu(\omega)$ is the complex modulus of the viscoelastic part from equation (4), and $\mathbf{q}$ and $\mathbf{F}$ are the displacement and the force vector respectively.

The equation of motion of the segment can be partitioned in the following manner :

$$\left\{ \begin{bmatrix} \mathbf{K}_{LL}^{(e)} & \mathbf{K}_{LR}^{(e)} & \mathbf{K}_{LI}^{(e)} \\ \mathbf{K}_{RL}^{(e)} & \mathbf{K}_{RR}^{(e)} & \mathbf{K}_{RI}^{(e)} \\ \mathbf{K}_{IL}^{(e)} & \mathbf{K}_{IR}^{(e)} & \mathbf{K}_{II}^{(e)} \end{bmatrix} + E_\nu(\omega) \begin{bmatrix} \mathbf{K}_{LL}^{(\nu)} & \mathbf{K}_{LR}^{(\nu)} & \mathbf{K}_{LI}^{(\nu)} \\ \mathbf{K}_{RL}^{(\nu)} & \mathbf{K}_{RR}^{(\nu)} & \mathbf{K}_{RI}^{(\nu)} \\ \mathbf{K}_{IL}^{(\nu)} & \mathbf{K}_{IR}^{(\nu)} & \mathbf{K}_{II}^{(\nu)} \end{bmatrix} - \omega^2 \begin{bmatrix} \mathbf{M}_{LL} & \mathbf{M}_{LR} & \mathbf{M}_{LI} \\ \mathbf{M}_{RL} & \mathbf{M}_{RR} & \mathbf{M}_{RI} \\ \mathbf{M}_{IL} & \mathbf{M}_{IR} & \mathbf{M}_{II} \end{bmatrix} \right\} \begin{bmatrix} \mathbf{q}_L \\ \mathbf{q}_R \\ \mathbf{q}_I \end{bmatrix} = \begin{bmatrix} \mathbf{F}_L \\ \mathbf{F}_R \\ \mathbf{0} \end{bmatrix}, \tag{6}$$

where coordinates $\mathbf{q}_L$,$\mathbf{q}_R$ and $\mathbf{q}_I$ denotes the physical degrees of freedom on the left boundary, on the right boundary and internal degrees of freedom respectively (as indicated by the corresponding subscripts). The internal degrees of freedom $\mathbf{q}_I$ are eliminated using a Guyan reduction [6], the relationship between the reduced and the original degrees of freedom can be written as:

$$\begin{bmatrix} \mathbf{q}_L \\ \mathbf{q}_R \\ \mathbf{q}_I \end{bmatrix} = \mathbf{B} \begin{bmatrix} \mathbf{q}_L \\ \mathbf{q}_R \end{bmatrix}, \tag{7}$$

where

$$\mathbf{B} = \begin{bmatrix} \mathbf{1} & \mathbf{0} \\ \mathbf{0} & \mathbf{1} \\ \mathbf{\Psi}_L & \mathbf{\Psi}_R \end{bmatrix}, \tag{8}$$

with $\mathbf{\Psi}_L = -\mathbf{K}_{II}^{-1}(\omega = 0)\mathbf{K}_{IL}(\omega = 0)$ and $\mathbf{\Psi}_R = -\mathbf{K}_{II}^{-1}(\omega = 0)\mathbf{K}_{IR}(\omega = 0)$ are the static boundary modes, and $\mathbf{K}(\omega = 0) = \mathbf{K}^{(e)} + E_0\mathbf{K}^{(\nu)}$, the latter is valid for the subscripts $LL, II, RR, LR, LI, RL, RI$ IR and IL.

Craig Bampton reduction followed by a dynamic condensation is generally more accurate than Guyan reduction when inertial forces exist, but requires inversions at each frequency step. Since the fixed interface modes of the beam section in our case are higher order modes with respect to the frequency range of interest (in this case from 10 Hz until 2000 Hz), the static condensation is more than sufficient for reducing the unit cell. In case the beam is not homogeneous along x direction, e.g. due to the presence of periodically placed resonators, Guyan reduction will no longer hold and a certain number of fixed interface modes must be taken into account in equations (7) and (8) in order for the reduced system to represent the same dynamics as the original one in the frequency range of interest, as for example applied in [21].

The condensed equation of motion can be written as :

$$\left\{ \begin{bmatrix} \tilde{\mathbf{K}}_{LL}^{(e)} & \tilde{\mathbf{K}}_{LR}^{(e)} \\ \tilde{\mathbf{K}}_{RL}^{(e)} & \tilde{\mathbf{K}}_{RR}^{(e)} \end{bmatrix} + E_\nu(\omega) \begin{bmatrix} \tilde{\mathbf{K}}_{LL}^{(\nu)} & \tilde{\mathbf{K}}_{LR}^{(\nu)} \\ \tilde{\mathbf{K}}_{RL}^{(\nu)} & \tilde{\mathbf{K}}_{RR}^{(\nu)} \end{bmatrix} - \omega^2 \begin{bmatrix} \tilde{\mathbf{M}}_{LL} & \tilde{\mathbf{M}}_{LR} \\ \tilde{\mathbf{M}}_{RL} & \tilde{\mathbf{M}}_{RR} \end{bmatrix} \right\} \begin{bmatrix} \mathbf{q}_L \\ \mathbf{q}_R \end{bmatrix} = \begin{bmatrix} \tilde{\mathbf{F}}_L \\ \tilde{\mathbf{F}}_R \end{bmatrix}, \tag{9}$$

where $\tilde{\mathbf{K}}^{(\mathbf{e})} = \mathbf{B}^T\mathbf{K}^{(e)}\mathbf{B}$, $\tilde{\mathbf{K}}^{(\nu)} = \mathbf{B}^T\mathbf{K}^{(\nu)}\mathbf{B}$, $\tilde{\mathbf{M}} = \mathbf{B}^T\mathbf{M}\mathbf{B}$ and $\tilde{\mathbf{F}} = \mathbf{B}^T\mathbf{F}$.

equation (9) can be written in terms of the dynamic stiffness matrix $\tilde{\mathbf{D}}$ as follows :

$$\begin{bmatrix} \tilde{\mathbf{D}}_{LL} & \tilde{\mathbf{D}}_{LR} \\ \tilde{\mathbf{D}}_{RL} & \tilde{\mathbf{D}}_{RR} \end{bmatrix} \begin{bmatrix} \mathbf{q}_L \\ \mathbf{q}_R \end{bmatrix} = \begin{bmatrix} \tilde{\mathbf{F}}_L \\ \tilde{\mathbf{F}}_R \end{bmatrix}, \tag{10}$$

where $\tilde{\mathbf{D}} = \tilde{\mathbf{K}}^{(\mathbf{e})} + E_\nu(\omega)\tilde{\mathbf{K}}^{(\nu)} - \omega^2\tilde{\mathbf{M}}$.

After applying Floquet-Bloch conditions, one obtains :

$$\mathbf{q}_R = \lambda \mathbf{q}_L, \tag{11}$$

and

$$\begin{bmatrix}\mathbf{q}_L & \mathbf{q}_R\end{bmatrix}^T = \mathbf{\Gamma}_R \mathbf{q}_L, \tag{12}$$

where $\mathbf{\Gamma}_R = \begin{bmatrix}\mathbf{I} & \lambda\mathbf{I}\end{bmatrix}^T$, $\mathbf{I}$ being the identity matrix and λ being the propagation constant.

The dynamic equilibrium of the segment holds the following equations :

$$\mathbf{\Gamma}_L \mathbf{F} = \mathbf{0}, \tag{13}$$

where $\mathbf{\Gamma}_L = \begin{bmatrix}\mathbf{I} & \frac{1}{\lambda}\mathbf{I}\end{bmatrix}$.

Pre-multiplying both sides of equation (10) by $\mathbf{\Gamma}_L$ and using equations (12) and (13), yields the classic quadratic eigenvalue problem of 1D wave propagation in terms of the propagation constant [23] :

$$[\lambda^2 \tilde{\mathbf{D}}_{LR} + \lambda(\tilde{\mathbf{D}}_{LL} + \tilde{\mathbf{D}}_{RR}) + \tilde{\mathbf{D}}_{RL}]\mathbf{q}_L = \mathbf{0}. \tag{14}$$

The frequency dependence is not an issue in this method as equation (14) is solved by fixing the frequency and calculating for the propagation constant.

3.2 Dispersion curves extraction method

A couple of works have been published to experimentally retrieve dispersion curves from vibrating structures. In [22] the in-homogeneous wave correlation method (IWC) was presented, that maximizes the correlation between the experimental displacement and a plane wave by adjusting the wave-number. This method has the edge of being applicable to 1D as well as 2D structures and has been compared to a spatial Fourier transform method for bending waves in beams in [25]. In the present paper, McDaniel's method [24] will be used to retrieve dispersion curves from a numerical noisy experiment. This method adjusts wave-numbers and wave-amplitudes of a postulated wave-field propagating in the structure with the reference response, and this is done at each frequency step. Contrary to other methods, the method does not require long structures with high damping so that a wave generated at one end is attenuated before it reaches the other end. However, it can be computationally expensive due to numerous parameters (wave numbers and wave amplitudes) that are optimized for. In the following, the latter method is applied to the treated beam depicted in fig. 1, the numerical displacements along the beam are polluted with noise and spatially sampled at 100 locations. The wave-field (to be fitted) in the structures is constructed by a finite set of waves that propagate back and forth and that decay due to the damping of the structure:

$$W(x,\omega) = \sum_r a_r(\omega) e^{-ik_r(\omega)x} + b_r(\omega) e^{-ik_r(\omega)(L-x)}, \tag{15}$$

where each r represents a distinct wave type that propagates in the structure with a complex valued wavenumber $k_r(\omega)$. The following minimization problem is run at each frequency step and provides the extracted dispersion curves :

$$\min_{k_r, a_r, b_r} \quad \sum_{samples} \left|\left| \frac{W - \tilde{W}}{\tilde{W}} \right|\right|^2 \qquad \forall r. \tag{16}$$

where $\tilde{W}$ are the reference displacements.

This method is applied to the cantilever treated beam case (see fig. 1). 2 percent of random noise (with respect to the wave's amplitudes) was added to the beam's displacement. Two wave types have been considered $r = 2$ corresponding to a propagating and evanescent wave (only two bending wave types exist in any 1D isotropic beam). The wave-number of the propagating wave is shown in fig. 3.

It is noteworthy that the treated beam is purposely chosen highly damped (see fig. 4) so as to show the advantages of the proposed viscoelastic parameter identification method. Starting from 600 Hz, the frequency response function shows a smoother behavior due to the high damping of the treated beam.

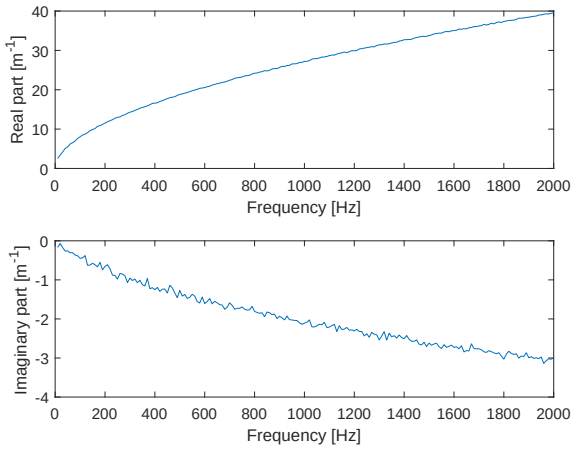

Figure 3: Real and imaginary wave-number of the propagating wave extracted from the treated beam using McDaniel's method

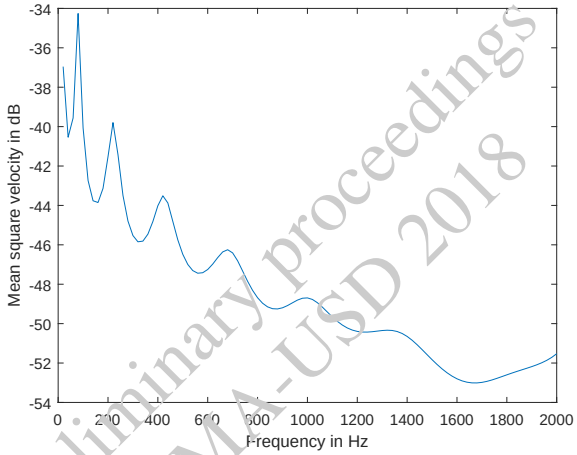

Figure 4: Mean square velocity of the treated beam shown in fig. 1 excited with a unit force.

4 Proposed identification inverse method

Solving the quadratic eigenvalue problem in equation (14) at multiple iterations can be computationally expensive, therefore, effort has been specifically focused on the construction of a surrogate model which will alleviate this issue. Surrogate models represent an approximation that is cheaper and more convenient to evaluate, than the underlying models they approximate. The most common use of surrogate models is to replace a known expensive computational model when a large number of repeated evaluations is required, e.g., for optimization or uncertainty quantification. Another common application is to obtain a continuous function from a fixed dataset, e.g., when the data is obtained experimentally. A third application is smoothing an underlying model with a lower order of continuity, perhaps to achieve differentiability for gradient-based optimization. In the following, a surrogate-based optimization is deployed to identify the viscoelastic parameters.

4.1 Surrogate model

Surrogate modeling approaches can be classified as interpolation (if the surrogate model matches the true function value at each point in the training dataset) or regression (if it does not). Regression methods smoothly approximate noisy data, and they include polynomials, splines, artificial neural networks (ANN), or

support vector regression (SVR). Interpolation methods attempt to smoothly and accurately fit non-spurious data, and they include inverse distance weighting (IDW), radial basis functions (RBFs), or kriging. These methods are extensively discussed in the literature in different applications e.g. see [26, 27, 28].

4.1.1 Radial basis functions

Radial basis functions (RBFs) are defined as linear combinations of basis functions, where each basis function depends on the distance from the prediction point to each training point. The coefficients in the linear combination are determined by solving a linear system that is typically dense. The radially varying basis functions are usually augmented with polynomial functions to capture the general trends.

In the following, the thin plate spline basis functions equation (17) are chosen because they have the edge of having no parameter that need to be tuned, whereas other basis functions do.

$$\psi_i(\mathbf{X}) = ||\mathbf{X} - \mathbf{X_i}||_2^2 \ln ||\mathbf{X} - \mathbf{X_i}||_2 \quad \forall i, \tag{17}$$

where $\mathbf{X_i}$ are the training points.

Prediction using the RBFs is given by :

$$k(\mathbf{X}) = \sum_i w_i \psi_i(\mathbf{X}) + \sum_j v_j p_j(\mathbf{X}), \tag{18}$$

where p_j is a polynomial function taken here as 1st degree polynomial, w_i and v_i are the unknown weights associated with the ith basis function and the ith polynomial trend function respectively.

In matrix notation, equation (18) can be written as :

$$\mathbf{k} = \mathbf{\Psi W} + \mathbf{PV}, \tag{19}$$

where $\mathbf{k}$ is a column vector of output training points $k(\mathbf{X_j})$ (wavenumbers), $\mathbf{W}$ and $\mathbf{V}$ are column vectors that consist of the coefficients w_j and v_j respectively, $\mathbf{\Psi}$ is the matrix $[\psi_i(\mathbf{X}_j)]_{ij}$, and $\mathbf{P}$ is the matrix $[p_i(\mathbf{X}_j)]_{ij}$, i denotes the row indices while j denotes the column indices. The training of RBFs consists of computing the weights by solving the following linear system :

$$\begin{bmatrix} \mathbf{k} \\ \mathbf{0} \end{bmatrix} = \begin{bmatrix} \mathbf{\Psi} & \mathbf{P} \\ \mathbf{P}^T & \mathbf{0} \end{bmatrix} \begin{bmatrix} \mathbf{W} \\ \mathbf{V} \end{bmatrix}. \tag{20}$$

A uniform sampling is used for the training points with a spacing of 10 points for each parameter.

It is note-worthy that we only focus on propagating waves with a decaying component (see fig. 3). The evanescent waves (their real part of the wave-number is smaller than their imaginary part) are not considered in the fitting.

4.2 Identification procedure

A set of three visco-elastic parameters (α, τ, E_∞) can be identified by solving the following minimization problem :

$$\begin{aligned} \min_{\mathbf{X}=(\alpha,\tau,E_\infty)} \quad & f(\mathbf{X}) = \sum_{frequencies} \left|\left| \frac{k'(\mathbf{X}) - \tilde{k}'(\mathbf{X})}{\tilde{k}'(\mathbf{X})} \right|\right|^2 + \left|\left| \frac{k''(\mathbf{X}) - \tilde{k}''(\mathbf{X})}{\tilde{k}''(\mathbf{X})} \right|\right|^2, \\ \text{subject to} \quad & 0 \leq \alpha \leq 1, \end{aligned} \tag{21}$$

where the prime and the double prime refer to the real and imaginary part of the wave-numbers respectively, k is the wave number constructed using the surrogate model presented in section 4.1, and $\tilde{k}$ is the propagating wave-number extracted from the numerical experiment explained in section 3.2.

The design variables that are optimized for are written in the following manner in order to efficiently span a broad range of values :

$$\begin{aligned} p_1 &= 10\alpha, \\ p_2 &= \log_{10}(\tau), \\ p_3 &= \log_{10}(E_\infty). \end{aligned} \tag{22}$$

It was noted during the numerical experiment that it is hard to identify the static modulus as the cost function, see equation (21), is not very sensitive to this parameter.

4.2.1 Two-parameter identification

In a first trial, the optimization is run on two parameters, the others being held constant. The cost functions with respect to two parameters are shown in fig. 5, fig. 6 and fig. 7. The results of the optimization are summarized in table 2, table 3 and table 4.

Parameters	Initial	Reference	Optimized
p_1	1.5	6	6.0001
p_2	-3.5	-6	-6.0011

Table 2: Numerical results for the case $\mathbf{X} = (\alpha, \tau)$

Parameters	Initial	Reference	Optimized
p_3	7	10	9.9981
p_2	-3.5	-6	-6.0001

Table 3: Numerical results for the case $\mathbf{X} = (E_\infty, \tau)$

Parameters	Initial	Reference	Optimized
p_3	7	10	9.9998
p_1	1.5	6	6.0011

Table 4: Numerical results for the case $\mathbf{X} = (E_\infty, \alpha)$

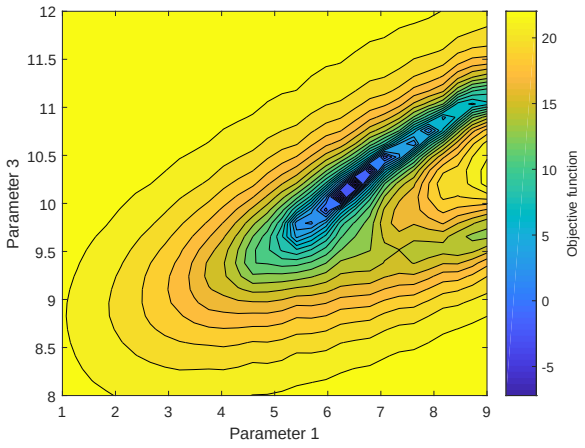

Figure 5: Logarithm of the objective function with respect to the parameters 1 and 3

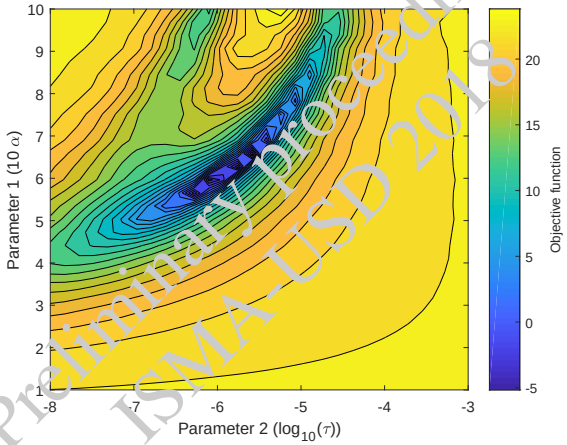

Figure 6: Logarithm of the objective function with respect to the parameters 1 and 2

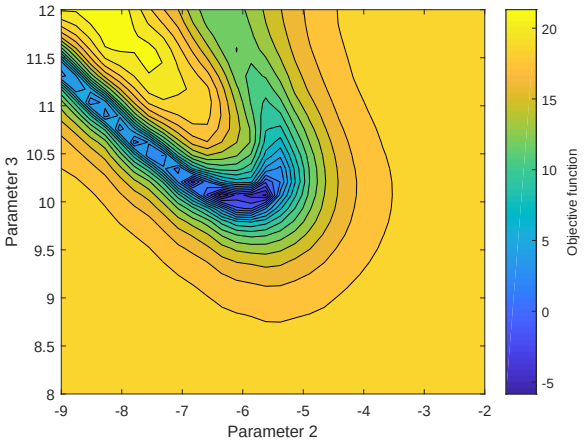

Figure 7: Logarithm of the objective function with respect to the parameters 2 and 3

A gradient-based optimization is deployed using Newton's method, the gradient and the Hessian are analytically calculated : exploiting the surrogate model previously built (see section 4.1). The present characterization technique has identified two-parameters at once in the frequency range of $[10\ 2000]$ Hz with 10 Hz increment, keeping the rest constant. The next section will treat the case of a three-parameter identification.

The cost function (see equation (21)), is not sensitive to the static modulus . This is depicted in figs. 8 to 10, showing horizontal or vertical lines indicating the value of the cost function is not considerably changing when varying the static modulus.

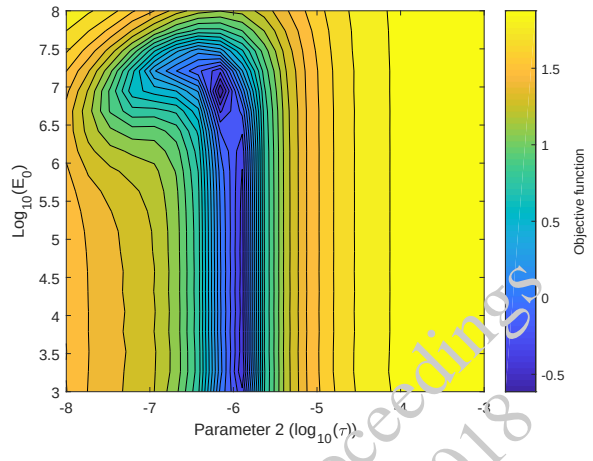

Figure 8: Logarithm of the objective function with respect to the parameters 1 and $\log_{10}(E_0)$

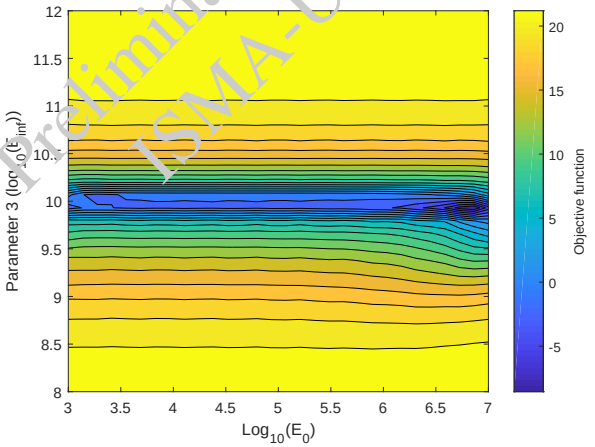

Figure 9: Logarithm of the objective function with respect to the parameters 3 and $\log_{10}(E_0)$

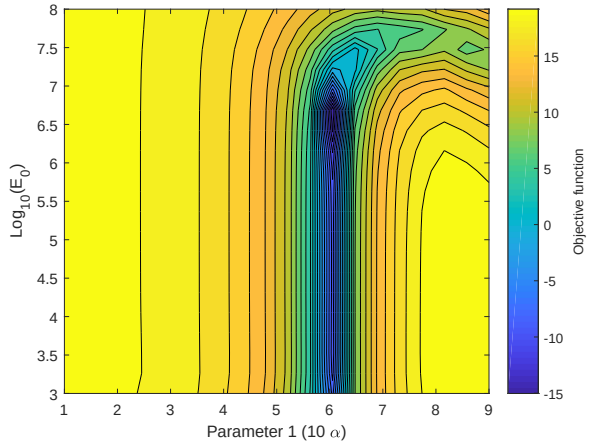

Figure 10: Logarithm of the objective function with respect to the parameters 2 and $\log_{10}(E_0)$

4.2.2 Three-parameter identification

Three parameters (E_∞, α, τ) can also be identified at once using this proposed method. The path of the optimization scheme is shown is fig. 11, the summarized results are given in table 5.

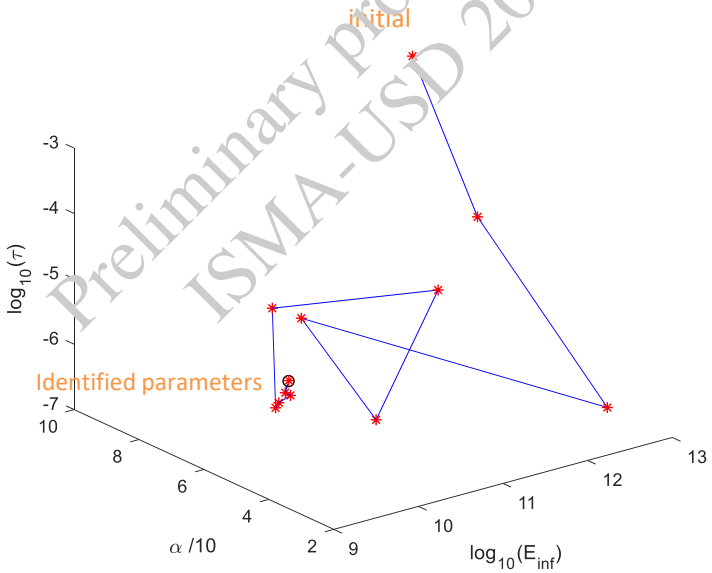

Figure 11: Path of the optimization convergence in the parameter space (E_∞, α, τ)

The identification of three parameters at once was successful using the proposed method. It is advisable to characterize E_0 first using static methods, and then plug it into this technique to retrieve the remaining parameters.

Parameters	Initial	Reference	Optimized
p_1	10	6	6.0001
p_2	-3	-6	-6.0011
p_3	13	10	9.9988

Table 5: Numerical results for the case $\mathbf{X} = (E_\infty, \alpha, \tau)$

5 Conclusion

This paper presents a dispersion-based characterization technique for identifying viscoelastic material properties. This method is applied to a highly damped beam and is able to characterize it over a wide frequency range. It is shown that, contrary to frequency response-function based inverse techniques, the proposed method does not loose its efficacy when dealing with highly damped structures. It actually makes the identification procedure easier as it is expected to capture more efficiently, the imaginary wave-number corresponding to the attenuation due to the added damping. Whereas the identification using the former method can become delicate because most of the material damping information is found at resonant frequencies levels, that most likely are not pronounced in case of high damping. However, the proposed method is not applicable to lightly damped structures as the signal to noise ratio of imaginary part of the extracted dispersion curves will be very low, which will make it difficult to extract the attenuating part of the propagating wave-number in a stable manner.

Acknowledgements

The research of T. Bourgana was funded by an Early Stage Researcher grant within the European Project VIPER Marie Curie European Joint Doctorates (GA 675441). The Research Fund KU Leuven is gratefully acknowledged for its support. E. Deckers is a post-doctoral fellow of the research foundation - Flanders. The research institute FEMTO-ST and Université de Bourgogne Franche-Comté, France, are gratefully acknowledged for their support. This research was performed in cooperation with EUR EIPHi (project ANR 17-EURE-0002).

References

[1] P. Butaud, E. Foltête, M. Ouisse. Sandwich structures with tunable damping properties: On the use of Shape Memory Polymer as viscoelastic core. *Composite Structures*, 153:401-408 , 2016.

[2] P. Butaud, M. Ouisse, V. Placet, F. Renaud, T. Travaillot, A. Maynadier, G. Chevallier, F. Amiot, P. Delobelle, E. Foltête, C. R. -Berriet . Identification of the viscoelastic properties of the tBA/PEGDMA polymer from multi-loading modes conducted over a wide frequency–temperature scale range. *Polymer Testing*, 69:250-258, 2018.

[3] J. D. Ferry. *Viscoelastic properties of polymers*. John Wiley and Sons, 1980.

[4] ASTM Standards E756-05. Standard test method for measuring vibration-damping properties of materials. American Society for Testing and Materials, West Consholocken, PA, 2010.

[5] T. J. Royston, Z. Dai, R. Chaunsali, Y. Liu, Y. Pend, L. R. Magin. Estimating material viscoelastic properties based on surface wave measurements: A comparison of techniques and modeling assumptions. *The Journal of the Acoustical Society of America*, 130(6):4126–4138, 2011.

[6] R. J. Guyan. Reduction of stiffness and mass matrices,*AIAA Journal*,3(2), 1965.

[7] Y. Sogabe, M. Tsuzuki. Identification of the dynamic properties of linear viscoelastic materials by the wave propagation testing. *Bulletin of JSME*, 29(254): 2410–2417, 1986.

[8] K. Ege, N.B. Roozen, Q. Leclere, R.G. Rinaldi. Assessment of the apparent bending stiffness and damping of multilayer plates; modelling and experiment. *Journal of sound and vibration*, 426:129–149, 2018.

[9] C. Pézerat, J.-L. Guyader. Force analysis technique: reconstruction of force distribution on plates. *Acta Acustica united with Acustica*, 86(2):322–332, 2000.

[10] N.B. Roozen, Q. Leclere, K. Ege, Y. Gerges. Estimation of plate material properties by means of a complex wavenumber fit using Hankel's functions and the image source method. *Journal of sound and vibration*,390:257–271, 2017.

[11] J.-L. Guyader, C. Cacciolati, Viscoelastic properties of single layer plate material equivalent to multilayer composite plate.*Proceedings of Inter-Noise*, 2007.

[12] D. Ross, E. E. Ungar, E. Kerwin, Damping of plate flexural vibrations by means of viscoelastic laminae.*Structural damping*,44-–87, 1959.

[13] D.A. Castello, F.A. Rochinha, N. Roitman, and C. Magluta. Constitutive parameter estimation of a viscoelastic model with internal variables. *Mechanical Systems and Signal Processing*,22:1840—1857, 2008.

[14] F. Renaud, J. -L. Dion, G. Chevallier, I. Tawfiq, R. Lemaire. A new identification method of viscoelastic behavior: Application to the generalized Maxwell model. *Mechanical Systems and Signal Processing*, 25(3):991–1010, 2011.

[15] S.-Y. Kim and D.-H. Lee. Identification of fractional-derivative model parameters of viscoelastic materials from measured frfs. *Journal of Sound and Vibration*, 324:570—586, 2009.

[16] Y. Shi, H. Sol, and H. Hua. Material parameter identification of sandwich beams by an inverse method. *Journal of Sound and Vibration*, 290:1234—1255, 2006.

[17] E. Zhang, J.D. Chazot, J. Antoni, and M. Hamdi. Bayesian characterization of young's modulus of viscoelastic materials in laminated structures. *Journal of Sound and Vibration*, 332:3654—3666, 2013.

[18] L. Rouleau, J.Deü, A. Legay. Inverse characterisation of frequency-dependent properties of adhesives. *Journal of Physics: Conference Series*, 744(1), 2016.

[19] L. Rouleau, B. Pluymers, W. Desmet. Characterisation of viscoelastic layers in sandwich lightweight panels through inverse techniques. *NOVEM - Noise and Vibration, Emerging Technologies*,2015.

[20] A. Van De Walle, L. Rouleau, E. Deckers, W. Desmet. Parametric model-order reduction for viscoelastic finite element models: an application to material parameter identifications. *Proceedings of the 22nd International Congress on Sound and Vibration*, 2015.

[21] R. F. Boukadia, C. Droz, M. N. Ichchou, W. Desmet. A Bloch wave reduction scheme for ultrafast band diagram and dynamic response computation in periodic structures. *Finite Elements in Analysis and Design*, 148:1-12, 2018.

[22] J. Berthaut, M.N. Ichchou, L. Jezequel, K-space identification of apparent structural behaviour, *Journal of Sound and Vibration*, 280(5):1125—1131, 2005.

[23] B. R. Mace, D. Duhamel, M. J. Brennan, L. Hinke, Finite element prediction of wave motion in structural waveguides, *The Journal of the Acoustical Society of America*, 117:2835–2843, 2005.

[24] J. G. McDaniel, W. S. Shepard, Estimation of structural wave numbers from spatially sparse response measurements, *The Journal of the Acoustical Society of America*, 108(4):1674–1682, 2000.

[25] B. Van Damme, A. Zemp, Measuring Dispersion Curves for Bending Waves in Beams: A Comparison of Spatial Fourier Transform and Inhomogeneous Wave Correlation, *Acta Acustica united with Acustica*, 104(2):228–234, 2018.

[26] D. Zhao, D. Liu, M. Zhu, A surrogate model for thermal characteristics of stratospheric airship, *Advances in Space Research*, 61(12):2989–3001, 2018.

[27] J. T. Hwang, J. R. R. A. Martins, A fast-prediction surrogate model for large datasets, *Aerospace Science and Technology*, 75:74–87, 2018.

[28] A. Nobari, H. Ouyang, P. Bannister, Uncertainty quantification of squeal instability via surrogate modelling, *Mechanical Systems and Signal Processing*, 60–61:887–908, 2015.